Millimeter Wave Dual-Polarized Semi-Passive Energy Detection Backscattering RFID

I-Ting Chen
School of Electrical and Computer Engineering
Georgia Institute of Technology
Atlanta, USA
ichen64@gatech.edu

Manos M Tentzeris
School of Electrical and Computer Engineering
Georgia Institute of Technology
Atlanta, USA
etentze@ece.gatech.edu

2024 IEEE Wireless Power Technology Conference and Expo (WPTCE) | 979-8-3503-4913-9/24/$31.00 ©2024 IEEE | DOI: 10.1109/WPTCE59894.2024.10557383

***Abstract*—This paper presents a dual-polarized semi-passive energy detection backscattering RFID at $28\,\mathrm{GHz}$. A 2 by 2 dual-polarized patch antenna array, a Wilkinson power combiner, a low noise FET switch, and a half-wave self-biased rectifier made of a MA4E2037 Schottky diode are designed and optimized on Rogers RO4350B substrate. The antenna is dual-polarized to separate energy harvesting/detection and backscattering features of the system. By adding the biasing load, the rectifier has a low turn-on input power level and can output $0.3\,\mathrm{V}$ at an input power of $-5\,\mathrm{dBm}$. It reaches the highest power conversion efficiency of $40.2\,\%$ with an input power of $12.2\,\mathrm{dBm}$. The rectifier provides a low voltage into a low-power op-amp that connects to an oscillator feeding into a low-noise FET switch for backscattering signal modulation at $270\,\mathrm{kHz}$. This RFID tag can operate up to $40\,\mathrm{m}$ with $75\,\mathrm{dBm}$ EIRP.**

***Index Terms*—Energy Harvesting, Millimeter Wave, Dual-Polarized, Backscattering RFID**

I. Introduction

As we move into the 5G and Internet of Things (IoT) era, technologies leveraging millimeter wave (mm-Wave) have presented great opportunities because of the nature of high data rates and high power density. These features make mm-Wave a promising technology for fast communication as well as wireless power transfer (WPT). For IoT applications, it is projected that the number of connected devices will exceed 29 billion by 2050 [1], which comes with a need for at least an equal number of power sources or batteries that cause outstanding waste and manpower for installation and replacement. WPT becomes a promising solution for realizing future IoT applications to avoid the burden of replacing and recycling used batteries. Therefore, knowing and identifying the power source presented in the environment is crucial to performing energy harvesting. Research has presented different mm-Wave radio frequency identification (RFID) tags that can be used to detect motions and orientation [2] [3] at $24\,\mathrm{GHz}$ as well as realizing leveraging the existing 5G network as a power grid for ambient mm-Wave energy harvesting [4] at $28\,\mathrm{GHz}$ while no discussion in leveraging RFID for energy source detection and identification.

This work aims to develop a sensitive mm-Wave rectifier and encode the presence and polarization information of the energy source into the backscattering signal through an RFID. [5] has presented a high-efficiency low-power rectifier at $24\,\mathrm{GHz}$ by using a shunt resistor load for diode self-biasing. This work is built upon the existing development in orientation detection RFID and sensitive rectifier in mm-Wave to achieve a dual-polarized semi-passive energy detection backscattering RFID at $28\,\mathrm{GHz}$.

II. Antenna Design and Evaluation

Inspired by [2] and [3], a dual-polarized antenna is proposed to separate energy harvesting/detection and backscattering functions by polarization. A 2 by 2 dual-polarized patch antenna array is carefully designed in Antenna Magus and optimized in CST Studio at $28\,\mathrm{GHz}$ on Rogers RO4350B substrate ($\epsilon_r = 3.66$ and $h = 254\,\mu\mathrm{m}$). The antenna array is designed with square patches to achieve dual polarization, and the patches are fed with microstrip feedlines with quarter-wave transformers for impedance matching. After optimization in CST studio, the boresight beam has an angular width of $49.3°$ and a very low sidelobe level of $-18.6\,\mathrm{dB}$. Figure 1 shows the antenna dimensions. The four feeding ports allow this antenna to transmit and/or receive RF signals in vertical or horizontal polarization. The work in this paper leverages this feature to transmit and receive RF signals for communication and backscattering purposes in one polarization and harvest/detect energy from the other polarization.

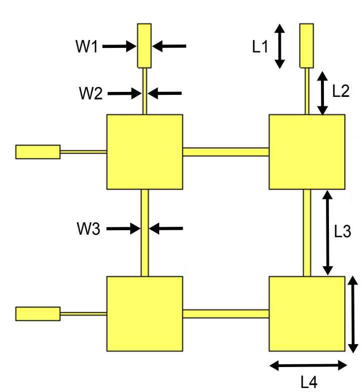

Fig. 1: 2 by 2 dual-polarized patch antenna array, where $L1 = 1.56\,\mathrm{mm}$, $L2 = 1.64\,\mathrm{mm}$, $L3 = 3.05\,\mathrm{mm}$, $L4 = 2.65\,\mathrm{mm}$, $W1 = 0.465\,\mathrm{mm}$, $W2 = 0.12\,\mathrm{mm}$, and $W3 = 0.26\,\mathrm{mm}$.

The designed 2 by 2 dual-polarized patch antenna array is fabricated with a masking inkjet printing technique followed by an etching process. The antenna evaluation is done in an anechoic chamber using a ShockLine MS46522B vector network analyzer (VNA) from Anritsu by connecting two antenna ports to the VNA while terminating the other two ports. This setup simulates the use case when a linearly polarized source is presented in the environment while another base station is in a perpendicular polarization. Figure 2 displays the simulated and measured realized gain from $-90°$ to $90°$ to boresight, with a maximum measured realized gain of $8.64\,\mathrm{dBi}$. It can be seen that the simulated and measured radiation patterns overlap each other, validating the antenna design.

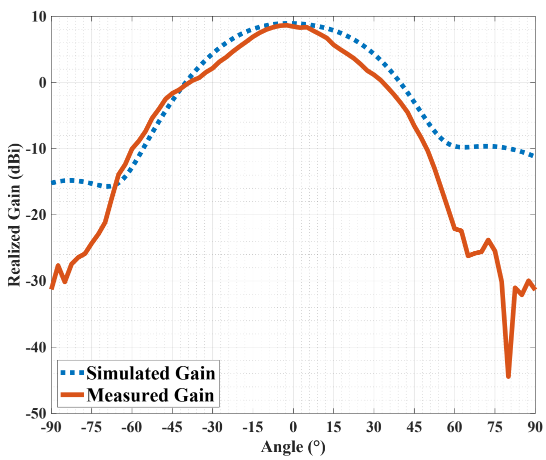

Fig. 2: 2 by 2 dual-polarized patch antenna realized gain against angle.

III. Energy Harvesting/Detection Design and Evaluation

A. Wilkinson Power Combiner

To take full advantage of the 2 by 2 patch antenna array, a 2 to 1 Wilkinson power (WPC) is designed and optimized at $28\,\mathrm{GHz}$ in CST Studio on the same substrate as the antenna to collect RF energy from both branches of the antenna. The WPC is designed based on the theory proposed in [6] to achieve a passive, reciprocal, and symmetric design. In addition, since each square patch on the antenna array is connected and presented as a short circuit in DC, a $100\,\mathrm{nF}$ capacitor is used as a DC block for isolating the DC voltage from the FET switches, that will be discussed later, and properly operating the entire system. The WPC design and optimization consider the capacitor to account for the additional loss. Figure 3 demonstrates the simulated and fabricated WPC, where port 1 is connected to the rectifier and ports 2 and 3 are connected to the two branches of the antenna. Figure 4 shows the measured signal transmission of the fabricated WPC. It shows that the WPC is properly designed to have an equal split of power ($3\,\mathrm{dB}$) between the two branches after de-embedding the transmission line loss. Two versions of WPC are fabricated, with and without the DC block capacitor, to accurately capture the extra loss caused by the capacitor and the soldering parasitic. It can be seen that the capacitor accounts for an additional $1.25\,\mathrm{dB}$ loss compared to the WPC without a capacitor.

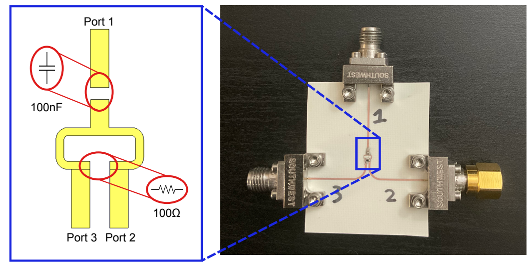

Fig. 3: Simulated and fabricated Wilkinson Power Combiner at $28\,\mathrm{GHz}$.

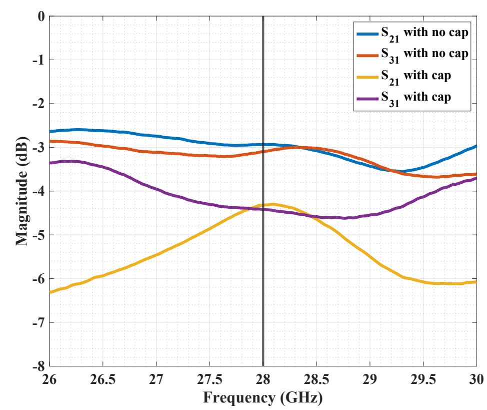

Fig. 4: De-embedded signal transmission characterization of the Wilkinson Power Combiner at $28\,\mathrm{GHz}$

B. Diode Selection and Modeling

The selection of the rectifying diode is crucial for efficient rectifier design, as the diode accounts for most of the rectifier circuit loss. The main parameters of a diode that affect the rectifier performance include junction capacitance (C_{j0}), series resistance ((R_s), turn-on voltage (V_j), and breakdown voltage (V_{br}). Considering these parameters, the diode chosen for this work is the commercially available and packaged gallium arsenide beam lead Schottky diode MA4E2037 from MACOM for implementation simplicity and performance stability. This Schottky diode has a series resistance of $4\,\Omega$, a turn-on voltage of $0.7\,\mathrm{V}$, and a breakdown voltage of $7\,\mathrm{V}$. To account for the parasitic from fabrication, which significantly affects the impedance matching and rectification performance in mm-Wave, the diode is characterized using through-reflect-line (TRL) calibration to obtain a realistic model. Figure 5 shows the realistic diode model for MA4E2037.

C. Self-Biased Rectifier

Reducing the required power needed for the diode is crucial in making an efficient rectifier. [5] has proposed a high-efficiency rectifier design at $24\,\mathrm{GHz}$ with a self-biased load

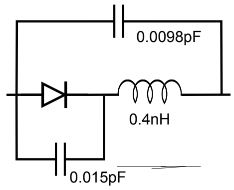

Fig. 5: Realstic MA4E2037 Schottky diode model.

to improve the rectification performance. The rectifier in this design, inspired by [5], utilized a shunt resistor connecting before the diode to realize a low-power rectifier at 28 GHz. 5 designs of rectifier with different biasing loads, $1\,\Omega$, $5\,\Omega$, $10\,\Omega$, $50\,\Omega$, and $100\,\Omega$, are simulated and compared to find the best biasing load in Keysight Advanced System Design (ADS) on the same Rogers RO4350B substrate. It is found in this work that the lower the biasing load, the better the rectification performance by evaluating the output DC voltage and power conversion efficiency, shown in Figures 6 and 7. It is noted that in these comparisons, the rectifier is only constructed with the biasing load and the diode for simplicity. Therefore, the output DC voltage and the power conversion efficiency are only to evaluate the trend when the biasing load changes and the rectifier is not yet optimized.

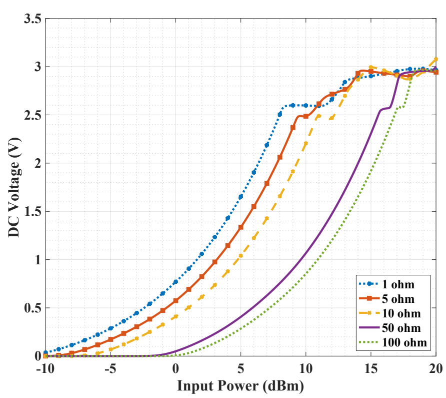

Fig. 6: Output DC voltage of rectifiers with different biasing loads.

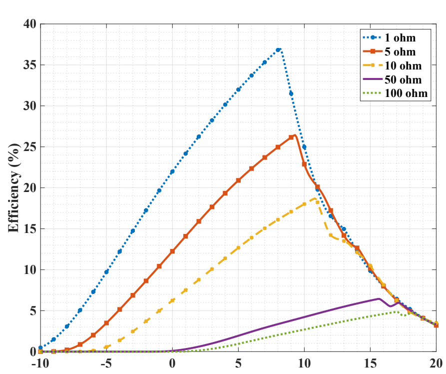

Fig. 7: Power conversion efficiency of rectifiers with different biasing loads.

Based on the rectification performance comparison, the biasing load chosen for this rectifier design is $1\,\Omega$. To terminate the fundamental and the second harmonics generated by the diode non-linearity when rectifying RF signals, two 60° radial stubs at a quarter wavelength at the two harmonic frequencies, 28 GHz and 56 GHz, are included in the design to provide short paths for the unwanted harmonics. Lastly, a 100 nF 560L104YTRN capacitor is used at the end of the rectifier to smooth the output DC voltage ripple. The final rectifier design with a single stub matching network is shown in Figure 8. In Figure 9, the optimal load to achieve the highest power conversion efficiency is $500\,\Omega$, and it has a low turn-on power at less than $-10\,\mathrm{dBm}$. Figure 9 shows that this rectifier can reach maximum efficiency of $40.2\,\%$ at an input power of $12.2\,\mathrm{dBm}$.

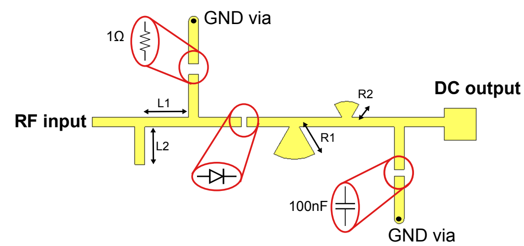

Fig. 8: 28 GHz half wave self-biased rectifier, where $L1 = 2.07\,\mathrm{mm}$, $L2 = 1.76\,\mathrm{mm}$, $R1 = 1.46\,\mathrm{mm}$, and $R2 = 0.68\,\mathrm{mm}$.

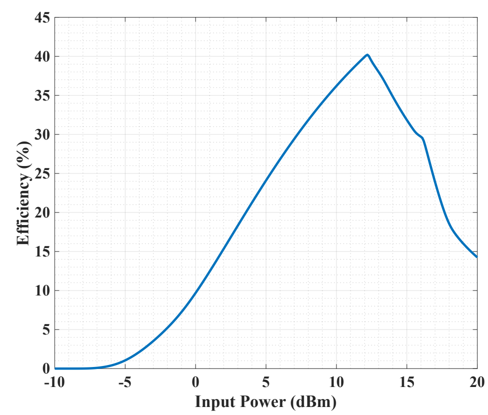

Fig. 9: Power conversion efficiency of the $1\,\Omega$ self-biased rectifier with a 500 ohm load.

IV. Backscattering RFID Design and Simulation

To perform RF signal backscattering with modulation at a center frequency of 28 GHz, two RF CE3520K3 FET switches are used for their low noise figure and low cost. The FET switch presents two different loads under biasing and non-biasing conditions. When the biasing voltage, 1 V, at the gate is present, the switch presents as a short circuit. On the other hand, when the biasing voltage is absent, the switch acts as an open circuit. This provides 2 conditions that can be encoded as present and absent of a perpendicularly polarized power source in the environment. The switch is characterized by comparing different radial stub lengths to optimize the signal phase and magnitude difference between the biasing and non-biasing conditions in Keysight ADS. Figure 10 displays the simulated and the fabricated FET switch. The measurement shown in Figure 11 indicates that the two conditions have a phase difference of 153.4° with the optimized radial length.

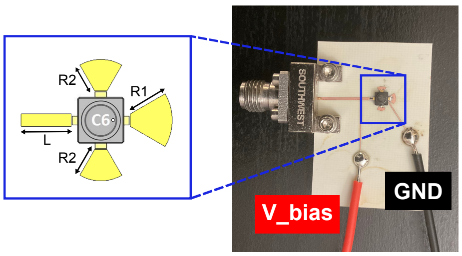

Fig. 10: Simulated and fabricated CE3520K3 FET switch characterization, where $R1 = 1.51\,\mathrm{mm}$, $R2 = 1.11\,\mathrm{mm}$, and $L = 1.88\,\mathrm{mm}$.

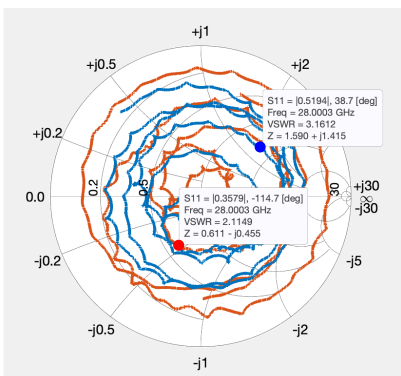

Fig. 11: CE3520K3 FET switch characterization on Smith Chart, where blue indicates non-biased condition and red indicates biased condition.

To supply a stable biasing voltage for the FET switch from the aforementioned rectifier and to increase the backscattering RFIS detection sensitivity, the baseband circuit consists of an MCP6042 rail-to-rail operational amplifier (op-amp) from Microchip Technology with a gain of 16 and a low-power TS3006 semi-oscillator to provide signal modulation at $270\,\mathrm{kHz}$, supplied by a solar cell. It is known that the higher the modulation frequency, the higher the power consumption, but the better the signal-to-noise ratio (SNR), as the modulated signal will be more distinguishable from the phase noise. $270\,\mathrm{kHz}$ is chosen for the modulation frequency as this is a good balance for this trade-off.

All the aforementioned components are connected in a dual-polarized energy harvester/detector backscatter RFID system, as shown in Figure 13. This backscattering RFID operates based on the status of the rectifier and the information of whether the rectifier is harvesting/detecting from a mm-Wave signal source with a perpendicular polarization of the transmission signal. The $28\,\mathrm{GHz}$ dual-polarized patch antenna array allows for RF signal backscattering and energy harvesting/detection in perpendicular polarizations. One side of the antenna branches is connected to a 2-to-1 WPC and into a half-wave self-biased rectifier while the other side of the branches is connected to a well-characterized low-noise FET switch to provide $270\,\mathrm{kHz}$ modulation for backscattering purposes. With the op-amp gain of 16, the rectifier has to reach $61\,\mathrm{mV}$ for the op-amp to generate $1\,\mathrm{V}$ to turn on the oscillator for FET biasing. Since the op-amp has an input impedance that is an open load, the rectifier is also characterized for this condition. Figure 12 shows that the rectifier can achieve the modulation threshold of $61\,\mathrm{mV}$ at an input power of $-8.5\,\mathrm{dBm}$. Considering the loss characterization of the WPC, this RFID tag can operate up to $40\,\mathrm{m}$ with $75\,\mathrm{dBm}$ EIRP from the transmitter.

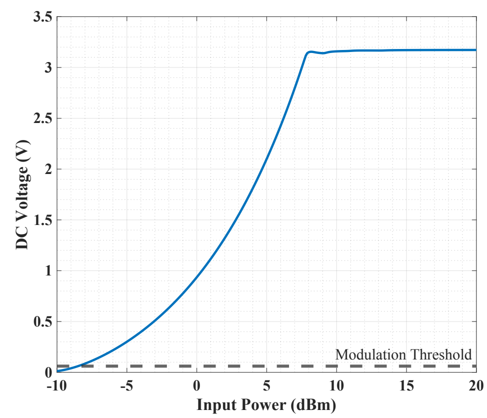

Fig. 12: Output DC voltage of the $1\,\Omega$ self-biased rectifier with an open load.

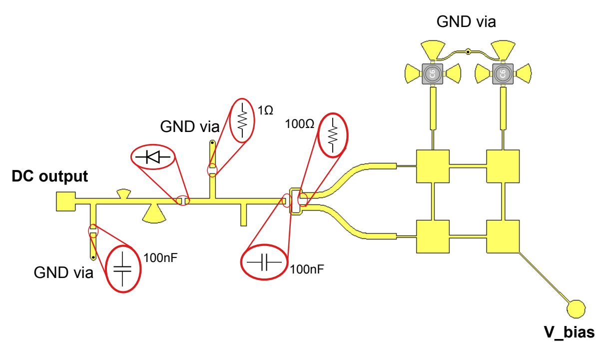

Fig. 13: Dual-polarized energy harvester and backscattering RFID layout, in size of $45\,\mathrm{mm} \times 23\,\mathrm{mm}$.

V. Conclusion

This work proposed a dual-polarized energy harvesting/detection backscattering RFID at $28\,\mathrm{GHz}$. This RFID will start backscattering with a modulated signal with a subcarrier of $270\,\mathrm{kHz}$ only when a cross-polarized signal source is present for energy harvesting in the environment. When the source is not presented, this RFID tag will retrodirectively backscatter a reflective signal from an open circuit. Therefore, it presents a useful tool for searching for and identifying a potential power source that is dual-polarized and, therefore, be overlooked by the transmitter. This work is only an energy detector due to the low power that the current rectifier can achieve, and it serves as a mid-step for a fully passive and energy-autonomous RFID tag. Current design operates up to $40\,\mathrm{m}$ with $75\,\mathrm{dBm}$ EIRP. With further exploration and optimization with a self-biased rectifier implemented with charge pumps, the design can be developed into a battery-less RFID tag for future IoT applications such as sensors operating for ultra-long range.

ACKNOWLEDGMENT

The authors would like to thank the National Science Foundation (NSF) for supporting this work.

REFERENCES

[1] L. S. Vailshery, "Iot connected devices worldwide 2019-2030," Jul 2023. [Online]. Available: https://www.statista.com/statistics/1183457/iot-connected-devices-worldwide/

[2] A. O. Adeyeye, J. Hester, and M. M. Tentzeris, "Miniaturized millimeter wave rfid tag for spatial identification and localization in internet of things applications," in *2019 49th European Microwave Conference (EuMC)*, 2019, pp. 105–108.

[3] C. A. Lynch, G. Soto-Valle, J. Hester, and M. M. Tentzeris, "mmids enter the 3rd dimension: A camera inspired broadbeam high-gain retrodirective backscatter tag," in *2023 IEEE/MTT-S International Microwave Symposium - IMS 2023*, 2023, pp. 1069–1072.

[4] A. Eid, J. G. Hester, and M. M. Tentzeris, "5G as a wireless power grid," *Scientific Reports*, vol. 11, no. 1, pp. 1–9, 2021.

[5] S. Ladan and K. Wu, "High efficiency low-power microwave rectifier for wireless energy harvesting," in *2013 IEEE MTT-S International Microwave Symposium Digest (MTT)*, 2013, pp. 1–4.

[6] E. Wilkinson, "An n-way hybrid power divider," *IRE Transactions on Microwave Theory and Techniques*, vol. 8, no. 1, pp. 116–118, 1960.